Chapter 2

Literature review

2. 1 Introduction

Chapter 2 comprises the extensive literature review and crystal structure of the ZrB_2, ZrC, and SiC ceramics. Furthermore, this literature review section explores the different processing routes utilized for synthesizing single-phase ZrB_2, as well as binary and ternary phase composites such as ZrB_2-ZrC, ZrB_2-SiC, and ZrB_2-ZrC-SiC. This chapter comprises reaction mechanisms and these materials' resulting properties and characteristics.

Additionally, the literature review addresses optimizing sintering procedures (pressureless sintering, spark plasma sintering, and hot pressing) and parameters used to enhance the density, homogeneity, and mechanical properties of UHTCs and their composites. The chapter provides an in-depth analysis of various sintering methods, with their advantages, limitations, and effects on the final material properties. By including this comprehensive literature review, the research study establishes a solid theoretical foundation and demonstrates a thorough understanding of the existing knowledge and advancements in the field. This section sets the stage for the subsequent chapters, providing a context for the research and highlighting the research gaps or opportunities the study aims to address.

2. 2 Crystal structure of ZrB_2/ZrC/SiC ceramics

ZrB_2 possesses a crystal structure that resembles the primitive hexagonal AlB_2 type. It belongs to the P6/mmm space group. The arrangement of the hexagonal closed-packed planes follows an ABABAB stacking sequence, alternating between transition metal (Zr) and boron (B) planes. Specifically, the Zr atoms occupy the 1a-lattice sites at coordinates (0, 0, 0), while the B atoms occupy the 2d sites at coordinates (1/3, 2/3, 1/2) and (2/3, 1/3, 1/2). In this structure, each Zr atom is constrained by six neighboring zirconium atoms in the same plane, while 12 equidistant boron atoms lie out of the plane. The boron atom is surrounded by three neighboring B atoms in its planes, which are, in turn, surrounded by six Zr atoms out of the planes [9,12,35], as shown in Fig. 2.1(a). The properties of ZrB_2 are affected by the combination of Zr-Zr, B-B, and Zr-B bonds [9].

ZrC, on the other hand, has a crystal structure known as a face-centered cubic (FCC) or rock salt structure. It belongs to the Fm3 m space group [36,37]. In this structure, the Zr atoms occupy the corner points of the cubes, while the interstitial sites are filled by the C atoms, as depicted in Fig. 2.1 (b).

SiC exhibits a variety of crystal structures known as polytypes. Certain polytypes of SiC adopt a Hexagonal closed-packed (HCP) system with the stacking of bilayers consisting of Si and C along the c-axis, as shown in Fig. 2.1 (c). Two possible stacking sites (A and B) exist on each Si-C bilayer (C). The lattice sites are either hexagonal (h) or cubic (c), depending on the polytype. For instance, cubic sites are present in 3C-SiC, 4H-SiC has one hexagonal and one cubic site, while 6H-SiC has one cubic and two hexagonal sites [38–41]. Table 2.1 presents the crystal structure, space group, lattice parameter, and atomic positions of ZrB_2/ZrC/SiC ceramics.

Table 2.1 Diversity of phases, crystal structures, space groups, and lattice parameters of ZrB_2, ZrC, and SiC

Materials	**Density (g/cc)**	**Crystal structure**	**Stacking sequence**	**Space group**	**Lattice parameter (Å)**			**Ref**
					A	B	c	
ZrB_2	6.1	HCP	ABABAB	P6/mmm (191)	3.170	3.170	3.533	[1,10]
ZrC	6.6	FCC		Fm3 m (No. 225)	4.72 4.689 a 4.72 b 4.698 c 4.68 d	4.72 4.689 4.72 4.698 4.68	4.72 4.689 4.72 4.698 4.68	[36]

SiC	3.21	2H-SiC	AB		3.07	3.07	5.05	[38]
	3.21	3C-SiC	ABC	T^2_d-F43m	4.36	4.36	4.36	
	3.21	4H-SiC	ABCB	C^4_{6v}-P6$_3$mc	3.07	3.07	10.05	
	3.21	6H-SiC	ABCACB	C^4_{6v}-P6$_3$mc	3.07	3.07	15.12	

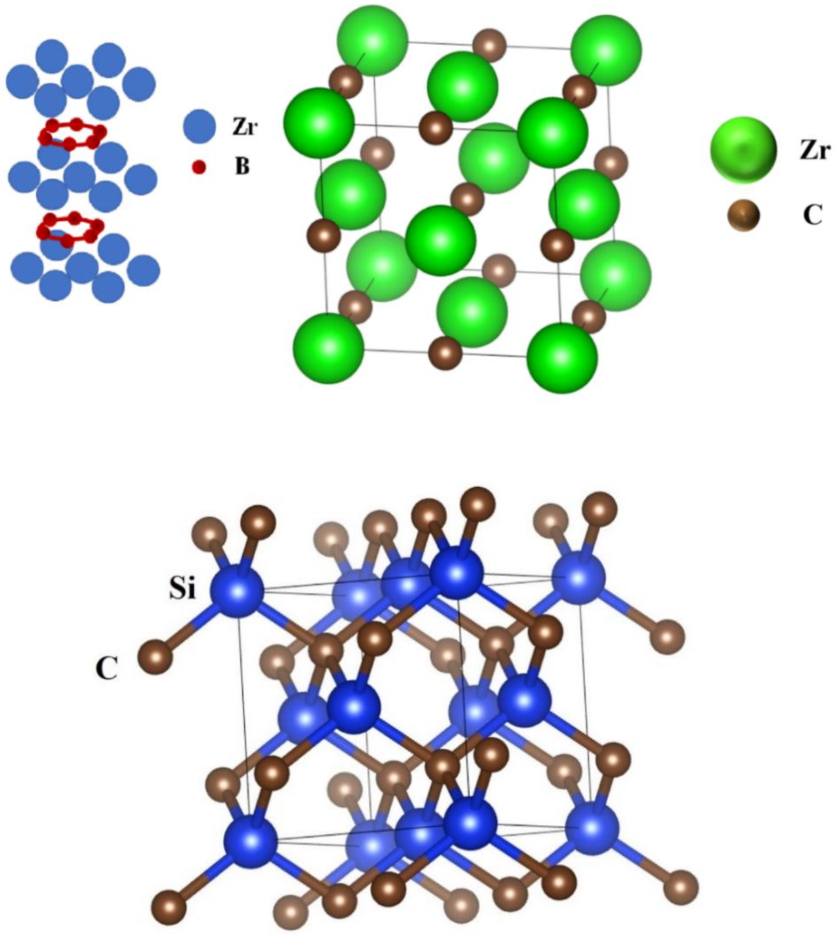

Fig. 2.1 Crystal structure of (a) ZrB_2 (b) ZrC (c) SiC

2. 3 Synthesis of ZrB_2, binary (ZrB_2–SiC and ZrB_2–ZrC) and ternary (ZrB_2–ZrC–SiC) composite

ZrB_2-based ultra-high temperature ceramic has been synthesized by various processing routes such as reduction processes such as borothermal [42–46], carbothermal [47–49], boro/carbothermal or boron carbide [50–54], molten salt [55–58], mechanochemical/metallothermic [59–64], sol-gel or solution-based method [65–68], self-propagating high-temperature synthesis/ direct reactive synthesis [69–73] and other processes [74–77]. However, researchers have encountered several challenges when synthesizing single-phase ZrB_2 ceramics using reduction, sol-gel, and different processing routes. One of the main issues is the presence of impurities, which can affect the purity and overall performance of the material. Achieving homogeneity, morphology, and controlling particle size in the synthesized ceramics is also challenging, as it requires uniform distribution of elements and phases. The high processing temperatures needed for synthesis also pose challenges regarding energy consumption, equipment compatibility, and material stability. The reaction kinetics during the synthesis process influences phase formation, crystallinity, and purity. Finally, cost considerations, including raw materials and equipment, add to the complexity of large-scale production.

To overcome these challenges, the researcher has focused on the effect of sintering aid on the particle size, homogeneity, densification, fracture toughness, oxidation resistance, and sinterability of ZrB_2 [19]. The processing route of binary such as ZrB_2–SiC [78–81] and ZrB_2–ZrC [82,83] and ternary (ZrB_2–ZrC–SiC) [84,85] composite. The presence of SiC in ZrB_2 can also control the grain size by removing oxide impurities on the surface and providing densification. The oxidation of SiC starts at 800°C, and the passive SiO_2 layer forms on the surface of the ZrB_2-SiC composite to control further oxygen diffusion up to 1600°C. The morphology of SiC in different shapes and sizes has also enhanced the mechanical strength in terms of fracture strength and fracture toughness. However, preferential oxidation of SiC under the passive SiO_2 layer is called the SiC-depleted layer. The high amount of SiC developed thermal residual stresses due to a mismatch of thermal coefficients [13,14]. The ternary composite of ZrB_2-based ceramic has excellent recession resistance compared to a binary system. Thus, another sintering additive, ZrC, is also incorporated in ZrB_2 ceramic to provide densification and oxidation resistance.

ZrB_2-SiC-ZrC ternary composites surpass two-phase composites in terms of performance enhancement. The thermo-mechanical properties of these synthesized composites critically depend on their morphology and the degree of densification achieved during the sintering process. The synthesis of these composite powders as a finer mixture poses a challenge, yet it is crucial for obtaining a high-performance finished product.

2.3.1 Reduction process

The reduction process is the most popular route to synthesize ZrB_2-based composite for large-scale production. Boron, boron carbide, magnesium, silicon, carbon (fiber and particulate), or a combination are reducing agents. The particle size and purity of reducing agents affect the purity of ZrB_2 ceramics.

Following reduction processes (endothermic nature) and reducing reactions are used for the synthesis of ZrB_2 powder:

2.3.1.1 Borothermal Reduction Process (BRP)

The BRP produces pure ZrB_2 ceramic with lower oxygen content (0.43 wt%), but this reduction takes place at higher temperatures (more than 1600°C) [42–46]. In this process, ZrO_2 and Boron are used as raw materials, as shown in the reaction (2.1). BRP is a very costly process because expensive boron is wasted in the form of boron oxide [42]. Various researchers have reported that the ZrO_2 co-exists with the ZrB_2 phase when processed at a lower temperature.

$$ZrO_2(s) + 4B(s) \rightarrow ZrB_2(s) + B_2O_2(g) \qquad (2.1)$$

2.3.1.2 Carbothermic Reduction Process (CRP)

The synthesis of ZrB_2 by the CRP involves ZrO_2 and B_2O_3 as cheap raw materials [47]. In this process, the boron atom replaces the oxygen atom in the ZrO_2 structure due to carbon's driving force, and the carbon source promotes a reduction reaction (2.2). Mishra et al. [70] have reported that the powder made from the CRP route at 1800°C has found 20% defect.

$$ZrO_2(s) + B_2O_3(s) + 5C(s) \rightarrow ZrB_2(s) + 5CO(g) \qquad (2.2)$$

2.3.1.3 Boro/carbothermal Reduction Process (BCTR) or Boron carbide Reduction Process (BCRP)

It is the most attractive method to synthesize low-cost ZrB_2 using less expensive raw materials. The reaction (2.3) occurs at temperatures higher than 1800°C with more than a 1 hr dwelling period.

$$2ZrO_2(s) + B_4C(s) + 3C(s) \rightarrow 2ZrB_2(s) + 4CO(g) \qquad (2.3)$$

Guo et al. [86] have studied that the ZrC phase is present along with ZrB_2 when the B_4C/ZrO_2 ratio is less, but with increasing B_4C content (20-25 wt%) in ZrO_2, the ZrC phase disappears with 0.7 wt% of oxygen presence at 1750°C. Another literature has been reported to optimize the stoichiometric ratio of ZrO_2 and B_4C for the lowest oxide and carbon impurity [52]. Similarly, Sonber et al. [54] investigated that the ZrB_2 phase has higher carbon and oxygen impurity even at 1200-1600°C. In reaction (2.4), some boron losses occur as boron oxide. Furthermore, with increasing temperature (1875°C), less than 0.5 % of carbon and oxygen content was present.

$$7ZrO_2(s) + 5B_4C(s) \rightarrow 7ZrB_2(s) + 3B_2O_3(s) + 5CO(g) \qquad (2.4)$$

Krishnarao et al. [78] show that ZrB_2–SiC composite has been synthesized using ZrO_2, B_4C, Si, and C as raw material rapid heating in an air furnace at 900°C and 1700°C. The ZrO_2 and ZrC impurities were present during pyrolysis at 1020-1500°C. The optimum molar ratio of ZrO_2/B_4C (2.5) without carbon addition and Si gives a 68.54% yield of ZrB_2.

In the two-step reduction process method, ultra-fine (10–40 nm) and highly homogeneous ZrB_2–SiC powder were synthesized by $ZrSiO_4$ and C as starting material. The starting precursor was mixed in high-energy ball milling and calcined at 1400°C and 1500°C for 1 hour under vacuum using SPS, as shown in the reaction (2.5).

$$ZrSiO_4 + 6C \rightarrow ZrC + SiC + 4CO \qquad (2.5)$$

Subsequently, resultant ZrC, residual ZrO_2, and B_4C are mixed and heated in the second step of the reduction process, which leads to forming ZrB_2 composite without borosilicate glass phase formation, as shown in the reactions (2.6) and (2.7).

$$ZrC + B_4C + ZrO_2 \rightarrow 2ZrB_2 + 2CO \qquad (2.6)$$

$$2ZrC + B_4C \rightarrow 2ZrB_2 + 3C \qquad (2.7)$$

The high synthesis temperature is also one of the disadvantages of the conventional boro/carbothermal process.

2.3.1.4 Molten salt reduction process (MS)

The direct molten salt reaction synthesized the ZrB_2 composite at low temperatures (600-900°C). In this method, potassium hexafluorozirconate (K_2ZrF_6) and potassium tetrafluoroborate (KBF_4) were used as starting materials for zirconium and boron sources, respectively [56]. In the above starting material, Al is used for in situ formations of hexagonal plate-like ZrB_2 particles. AlB_2 and Al_3Zr phases are present at lower temperatures in the final synthesized powder, but with increasing temperature, they disappear entirely, as shown in the reaction (2.8). The particle size and distribution are uniform due to aluminum's reduced starting material by the formation of the salt mixture [56].

$$AlB_2 + Al_3Zr \rightarrow ZrB_2(s) + 4Al \quad (2.8)$$

A less expensive raw material such as ZrO_2 and B_2O_3 with reducing agents such as Mg, Al, and Si makes unwanted oxide products that are removed by acid leaching, obtaining highly pure ZrB_2 powder shown in the reaction (2.9).

$$ZrO_2(s) + B_2O_3(s) + Mg\ (Al, Si)(s) \rightarrow ZrB_2(s) + MgO\ (Al_2O_3, SiO_2)(s) \quad (2.9)$$

2.3.1.5 Mechanochemical/Metallothermic reduction process (MCRP/MTRP)

The MTRP is employed to produce nanocrystalline ZrB_2 powder. This intricate process is executed at remarkably low synthesis temperatures, showcasing precision and efficiency in creating the desired material. Bai et al. [59] synthesized ZrB_2 powder using $ZrCl_4$, B, and Mg as raw material, as shown in the reaction (2.10). A similar route follows by using ZrO_2, $Na_2B_4O_7$, and Mg powders as starting raw materials for synthesizing nano ZrB_2 powder, as shown in the reaction (2.11). This reaction occurred at 1200°C, resulting in a 300-400 nm particle size obtained after acid leaching [64]. $Na_2B_4O_7$ and Mg promote the complete conversion of ZrO_2 into ZrB_2 powder. Mg and MgO were separated, and pure ZrB_2 powder was obtained [61].

$$ZrCl_4 + B + 2Mg \rightarrow ZrB_2 + 2MgCl_2 \quad (2.10)$$

$$Na_2B_4O_7 + 2ZrO_2 + 10Mg \rightarrow 2ZrB_2 + 10MgO + Na_2O \quad (2.11)$$

Similar to ZrB_2-based ceramic, ultrafine ZrB_2–SiC composite was synthesized using $ZrSiO_4$, B_2O_3, activated carbon, and Mg powder as a starting material at 1200°C shown in reaction (2.12), which was at least 200°C lower than the conventional methods[87].

$$ZrSiO_4(s) + B_2O_3(s) + C(s) + 7Mg(s) \rightarrow ZrB_2(s) + SiC(s) + 7MgO(g) \quad (2.12)$$

Furthermore, the ZrB_2–SiC–ZrC composite was synthesized by the MTRP using $ZrSiO_4$, B_2O_3, C, and metal (Mg, Al) in high-energy ball milling. Aluminum and magnesium are reducing agents, but aluminum cannot reduce the system, and production becomes amorphous in 10 h milling. This problem is resolved by Mg metal powder, which can reduce the boron oxide and $ZrSiO_4$ [88].

2.3.2 Solution-based or sol-gel method (SG)

The sol-gel method prepares highly pure and nano-size ZrB_2-based composite powder. The principal advantage inherent in the sol-gel process lies in its ability to achieve homogeneity in phase and chemical stability within ZrB_2-based ceramics. The sol-gel method arises from the initial synthesis procedure wherein the starting raw materials undergo interactive processes, ensuring a uniform and chemically stable composition in the resulting ceramic material. For example, Yan et al. [89] synthesize ultrafine (100-400nm) ZrB_2 powder by using zirconium oxychloride ($ZrOCl_2.8H_2O$), boric acid (H_3BO_3) and phenolic resin (as carbon source) using as raw material at 1500°C for 20-60 min with low oxide impurity. Similarly, Huiming et al. [67] synthesized ZrB_2 powder by sorbitol-modified sol-gel method using zirconium n-propoxide ($Zr(OPr)_4$) and boric acid, as a zirconium and boron source, and sorbitol as a carbon source. In reaction with H_3BO_3, sorbitol forms a chelate complex network structure that promotes the carbothermal reduction reaction at 1450°C. It is a faster and more energy-saving process to synthesize nano ZrB_2 ceramics material. The above researcher has concluded that the solution-based method is effective for low-temperature synthesis with fine ZrB_2 particles.

Along with these benefits, controlling particle size and morphology is essential, as irregular shapes or large particles can impact the material's densification during sintering. The researchers focused on improving synthesis techniques by utilizing other additives. Wang et al. [90] synthesized ZrB_2-SiC powder depending on the starting materials of zirconium n-propoxide tetraethyl orthosilicate, boric acid, acetic acid (AcOH), and sucrose by two-step sintering technique. Sucrose acts as a pyrolyzed carbon source. AcOH acts as a chemical modifier, so under natural conditions, metal oxide reactions take place. In the primary step, the sample is heated from 800°C to 1200°C at the rate of 3°C /min and held at 1200°C for 2 h; subsequently, the ZrB_2-SiC phase appears at 1550°C at 2°C /min and kept for 2 h. Recently, Ang et al. [91] synthesized ZrB_2-ZrC composites using $Zr(OR)_4$, sucrose, H_3BO_3, glacial acetic acid, polyvinylpyrrolidone, N-di-ethyl formamide at 1800°C. The carbothermal reduction occurred on the surface of ZrB_2 to form a nano ZrC phase (200 nm) by removal of ZrO_2 at 1450°C. The monolithic ZrB_2 sample has 82% theoretical density, but with the addition of ZrC in ZrB_2, the theoretical density is above 98%, depending upon the mixture. Furthermore, porous ZrB_2/ZrC/SiC ceramics were also synthesized via the sol-gel method and catalyst-assisted pyrolysis at 1400°C in argon flow (1 L/min) for 1 h with a heating rate of 10 °C/min. The short and tangled SiC whiskers have been growing in the interior portion of the porous ZrB_2/ZrC/SiC ceramics due to limited growing space, but on the surface of ZrB_2/ZrC/SiC ceramics, long and straight SiC whiskers have been formed [92]. ZrB_2-based composite ferrous chloride ($FeCl_2$) acts as a catalytic iron source for the growth of silicon carbide whiskers [68]. Recently, Liu et al. [85,93] developed nano-size ZrB_2–ZrC–SiC nanopowders at 1500°C for 2h by using $ZrOCl_2 \cdot 8H_2O$, H_3BO_3, TEOS, and glucose as a raw material shown in Fig. 2.2.

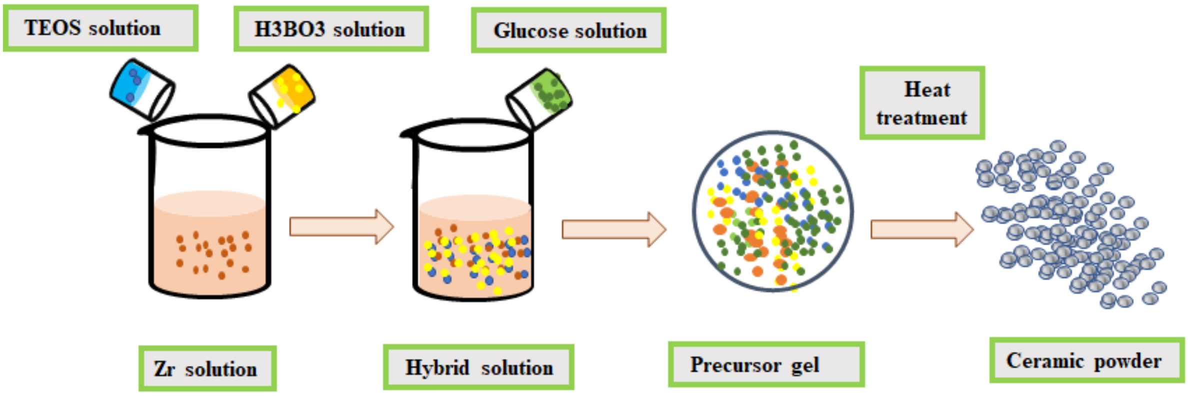

Fig. 2.2 Systematic diagrams of sample preparation by sol precursor method [67]

2.3.3 Self-propagating high-temperature synthesis (SHS)/ direct reactive process

The synthesis of highly pure ZrB_2 powder involves a self-propagating high-temperature process. This process results from the direct reaction between elemental boron and zirconium powder, occurring at lower temperatures and in shorter durations. The exothermic reaction (2.13) demonstrates this synthesis. SHS process includes a higher heating and cooling rate, which results in the creation of defect concentration. Mass transfer at lower sintering temperatures is essential in physical and chemical phenomena. Reducing sintering temperature provides the potential of zirconium diboride for excellent wear resistance, oxidation resistance, and ablation resistance at higher temperatures. Camurlu and Maglia et al. [72] have developed nanosized ZrB_2 powder using Zr and B as starting materials. 10–50% NaCl decreasing the adiabatic temperature of the reactions, reaction wave velocity, particle size, and average crystal size of the formed ZrB_2.The materials are synthesized in a reducing atmosphere to minimize the oxide impurity in ZrB_2 powder [73]. Mechanical activation-assisted self-propagating high-temperature synthesis is beneficial over another method due to its low cost and simple synthesis procedure.

$$Zr(s) + 2B(s) \rightarrow ZrB_2(s) \qquad (2.13)$$

2.3.4 Chemical vapor deposition (CVD)

This method uses zirconium and boron as a precursor to form ZrB_2 coating by the vapor phase reaction method. Reaction (2.14) shows that $ZrCl_4$ and BCl_3 are the most attractive percussor materials, and hydrogen is a reducing agent [74,75]. This reaction occurs at low temperatures for thin film. Although it requires a complex machine setup, the processing cost is high. The deposition rate increases with the hydrogen concertation in the gas mixture and is also influenced by increasing temperature.

$$ZrCl_4 + 2BCl_3 + 5H_2 \rightarrow ZrB_2 + 10HCl \qquad (2.14)$$

The synthesis of ZrB_2 films via the vapor phase deposition method requires only Zirconium borohydride [$Zr(BH)_4$] as a raw material at a low-temperature range of 100- 270°C with attractive mechanical and electronic properties. Reich et al. [77] deposited ZrB_2 coating in the 150–400°C temperature range using pre-requisite $Zr(BH)_4$.

2. 4 Sintering of ZrB_2, binary (ZrB_2–ZrC and ZrB_2–SiC) and ternary (ZrB_2–SiC–ZrC) composite

The sintering of ZrB_2-based ceramics and its composite through a conventional pressure-less sintering route [94–96], but it usually takes a very high sintering temperature to get monolithic ZrB_2-dense ceramic. These ceramics are tough to sinter due to covalent bonds, high melting points, low self-diffusion, and an oxide layer on the particle's surface [11]. Accordingly, non-conventional techniques, i.e., hot pressing [54,97,106–115,98,116,117,99–105] and spark plasma sintering [46,118,127–130,119–126], provide dense ZrB_2 ceramic for ultra-high temperature application. At high sintering temperatures, the grain growth of particles is very high, so the density is near the theoretical density, leading to poor mechanical properties

[131]. For monolithic materials, the equation (2.15) describes the relation between sintering time and average grain size [1];

$$G = GO + Kt \tag{2.15}$$

Where GO is the initial grain size, G is the average grain size, t is the sintering time, and n is the grain growth coefficient.

At lower temperatures, the grain growth and grain growth coefficient are hindered by the pores at grain boundaries. In contrast, grain growth is enhanced, and sintered density is increased by eliminating the surface pores, leading to ion transfer at a higher temperature. High sintered density and low particle size are compulsory for better mechanical properties. Several sintering additives increase densification without deteriorating the mechanical and physical properties**.** They also promote sintering at low temperatures and work as reinforced materials. This section consists of both conventional and advanced sintering techniques. Traditional sintering techniques, such as pressureless and hot pressing, and advanced techniques, like spark plasma, flash, laser, reactive, and microwave, have been discussed. This section mentions the sintering methods with their merits and demerits. It also analyzed the sintering and additive effects on mechanical properties (such as fracture toughness and strength), physical properties (density, grain size), and microstructure. The sintering process mentioned into the following types:

2.4.1 Pressureless sintering

Pressureless sintering is a conventional technique to produce dense, compact ZrB_{2}-based ceramic and composite. A uniaxial pressing machine has pressed the large and complex shape geometry at a high temperature and controlled atmosphere. The sintering temperature for pressureless sintering is usually 0.70 Tm (melting temperature) for higher density composite.

The densification parameter and mechanical properties depend upon the grain growth, which is affected by sintering temperature, sintering time, and sintering additive. Full densification of ZrB_2-based ceramic requires a longer duration at high sintering temperatures. The ZrB_2-based ceramics at 2150°C for 3 h sintering temperature could densify only up to 72%. But when the sintering time increases from 3 to 9h, the density improves to 98%. Due to increased holding time, substantial grain growth can be obtained from ~9 µm to ~30 µm, resulting in decreased mechanical properties compared to the hot-pressed technique. The mechanical properties such as hardness and flexural strength are 14.5 GPa and 444 MPa, respectively, possessed during pressureless sintering, which is relatively lower than hot-pressed hardness and flexural strength: 23 GPa and 565 MPa, respectively.

The mechanical properties decrease due to the larger grain size developed during pressureless sintering. Also, the anisotropic nature of the hexagonal crystal structure may contribute to the reduction of hardness with the formation of internal thermal stress in a crystallographic direction. The elastic modulus and flexural strength can be decreased due to the 2 vol% porosity in the sintered samples. The particle size is reduced by attrition and spex milling, resulting in increased surface area. The increased surface area increases the driving force for sintering by increasing point defect and dislocation, increasing densification [132]. In the pressureless sintering technique, the starting powder and the additive are mixed and cold-pressed inside the die with a particular amount and appropriate pressure to get the desired compact shape. The sintering additive reacted with the oxide impurities (ZrO_2 and B_2O_3) present on the surface of the raw material and enhanced the densification of the ZrB_2 composite. The main sintering additives are SiC [95], B_4C [133], C [134], and WC [135]. Adding 4 wt % B_4C provides a highly dense ZrB_2-based compact at 1850°C for 1h without external pressure [135].

Similarly, 4% WC provides 95% relative density of ZrB_2 composite sintered at 2050°C for 240 min [135]. An additional amount of B_4C restricts grain growth during sintering [135]. Mashhadi et al.[95] have reported that adding 10 wt% of nano and 15 wt% of micro-sized SiC in ZrB_2 powder improves densification. The relative density of ZrB_2 ceramic increased by adding nano and micro SiC. The ZrB_2–10 wt% SiC composite was sintered at 2200°C for 1h for maximum density (98 %) and high hardness (15.02 GPa) for nanoparticles. Such observation indicates that the sintering temperature range is 1500-2300°C for high densification of ZrB_2-based ceramic. In the case of a high sintering range, abnormal grain growth enhances micro-cracks inside the ZrB_2 composite due to coarsening of grains. Grain boundary cracking occurs when the grain size is beyond the critical limit.

In contrast, finer grain size is less susceptible to cracking during cooling. The abnormal cracks and significant stress are created inside the composites due to their brittle nature. Furthermore, ZrB_2-based ceramics have a non-cubic crystal structure, so high thermal expansion anisotropy may also cause spontaneous micro-cracks. According to the earlier discussion, high sintering temperature in pressureless sintering creates significant problems due to melting or evaporation of low melting components, leading to microstructure cracking.

Pressureless reactive sintering

Pressureless reactive sintering is an attractive technique because it can sinter at a relatively lower temperature and time with lesser impurity and good sinter density. In this method, an in-situ reaction occurs during heating; subsequently, holding precursor powder leads to densification. Brochu et al. [136] have reported that ZrB_2 ceramic can get 95% of relative densities with shock compaction and pressureless reactive sintering at 1600-2000°C. In another work, Brochu et al. [132] reported that ZrB_2 ceramic had been prepared by hand mixing (mortar) and high-energy milling (spex) of Zr and B as a starting material. The apex milled samples have 66-79%, and mortar mixed samples have 58-70% of relative theoretical densities after pressureless reactive sintering at 1800°C, 2000°C, and 2200°C without providing driving force compared with attrition milled.

Table 2.2 The sintered density, grain size, and mechanical properties of ZrB_2 and ZrB_2-based composite via pressureless sintering technique

Materials Composition	Sintering Condition	Microstructural Phases	Sinter-density (as% ρth)	Hardness (GPa)	Fracture Toughness (MPa m½	Flexural strength (MPa	Refs.
Zr+B (RPS) 325 mesh	1600°C/60 min	ZrB_2	71.3	19.4±0.4	-	-	[136]
	1800°C/60 min		71.9	17.2±0.6			
	2000°C/60 min		71.1	13.7±0.6			
ZrB_2 (200 nm) SiC (0.5 µm)	2250°C/120 min	ZrB_2–20 wt% SiC	97.7	14.82	5.39	-	[137]
ZrB_2: LPCS (4:1)	1600°C/ 120 min	ZrB_2–SiC	77	-	-	-	[94]
	1800°C/ 120 min		99				
	1800°C/ 120 min		95				
	2000°C/ 120 min		87				
ZrB_2, SiC micro	2200°C/ 60 min	ZrB_2–15 wt% SiC	96	14.08	-	-	[95]
ZrB_2, SiC nano		ZrB_2-10 wt% SiC	98.12	15.02	-	-	
Zr(40 µm) ,B4C (8 µm) ,Si(40 µm	1500°C/60 min then 1900°C 1hr	ZrB_2–ZrC–SiC	88.4	10.54	3.78	204 ± 5	[96]
	1000°C/60min then 1700°C/60 min		99.6	20.22	6.70	526 ± 9	

2.4.2 Hot pressing

Hot pressing is the most popular technique for obtaining densified ZrB_2-based ceramics and composites by applying external pressure at a sintering temperature. The mechanical properties of hot-pressed ZrB_2-based ceramic have better properties than pressureless sintering, which takes a lower temperature than pressureless sintering. It involves hydraulic uniaxial pressure and temperature simultaneously during the densification of powder by using a graphite heating element. ZrB_2 powder is milled in attrition milling to obtain less than 2 μm size powder. The milled powder is filled in a die and heated to the desired temperature in a vacuum/ argon atmosphere, and then uniaxial pressure is applied, as shown in Fig. 2.3. The better mechanical properties of the hot-pressed compact are due to a finer microstructure and fine grain size. The maximum density and fine grain size were achieved by adjusting hot pressing parameters such as applied pressure, sintering temperature, time, and atmosphere [98,99,109–117,100–105,107,108]. The fine grain size provides a highly dense structure during pressure-assisted sintering. Neuman et al. [99] fabricated ZrB_2-based ceramics by uniaxial hot pressing at 2100-2150°C with a 30-120 min holding at 32 MPa. The density of ZrB_2 ceramics ranged from 96.7 to 97.8% for 30 to 120 min, respectively, at 2150°C. Also, the mechanical properties of the specimen are a function of grain size and relative density. The ZrB_2 ceramics hot-pressed at 2150°C for 30 min consisted of the highest strength (400 MPa) and highest toughness (2.3 MPa $m^{1/2}$), while the material hot-pressed at 2150°C for 120 min had the highest modulus (510 MPa) and highest hardness (14.4 GPa) due to its higher density (97.8%). The sintered density of monolithic ZrB_2 ceramic is nearly equal to the theoretical sintered density at only extremely high sintering temperatures. The addition of nano-sized SiC particles improved the particle size as well flexural strength even in oxidation atmosphere/condition.

Furthermore, Guo et al. [104] have fabricated intergranular and intragranular nano-sized SiC particles in the ZrB_2 matrix via vacuum hot-pressing at 2000°C for 60min and under uniaxial pressure of 30 MPa. The nano SiC addition improves the oxidation resistance before and after exposure to dry air at 1400°C for 10 h. As received, the nano ZrB_2-SiC composite has 608 MPa 4-Point flexural strength, more significant than the micro ZrB_2-SiC composite (531 MPa). Similarly, post-exposed at 1400°C in dry air, it has 700 MPa 4-point flexural strength, which is more significant than micro ZrB_2-SiC composite (506 MPa). The hot-pressed laminated ZrB_2–SiC ceramic was developed by Zhou et al. [106] at 1950°C and 30 MPa for 60 min in an Ar atmosphere. The mechanical properties of laminated ZrB_2–SiC ceramics are higher than monolithic ceramics. The flexural strength and fracture toughness increase from 517 to 960 MPa and 5.6 to 8.8 $MPa{\cdot}m^{1/2}$, respectively, as the transition is made from monolithic to laminated ZrB_2–SiC ceramic. Recently, Nguyen et al. [138] examined the sintering governing mechanism of hot-pressed ZrB_2–SiC ceramic at different temperatures. At a low temperature of 1650°C, particle rearrangement and fragmentation promoted densification mechanisms.

The monolithic ZrB_2 ceramic grain growth is faster with temperature, but with ZrC and SiC, grain growth results in the most stable microstructure. Liu et al. [117] have reported the role of SiC and ZrC addition in hot-pressed ZrB_2-based ceramic. The ZrC and SiC grains are interconnected with significant phase ZrB_2 at 3-4 grain junctions, which restrict each other's grain growth. Three-phase ceramic exhibits more grain boundaries, so the diffusion path is more complex than two-phase ceramic. Therefore, grain growth would be more difficult in three-phase ceramics. The simultaneous addition of ZrC and SiC was beneficial for obtaining the homogenous and finer microstructure of ZrB_2-based ceramics, as shown in Fig. 2.3. Also, the thermal residual stress of ZrB_2–SiC–ZrC (400 MPa) is less than compared to ZrB_2–SiC (800 MPa) due to plastic deformation of ZrC. In ZrB_2–ZrC-based ceramic, crack deflection around the ZrC grain was the primary toughening mechanism. The main limitation of the HP method is the preparation of complex shapes and geometry due to the application of uniaxial pressing.

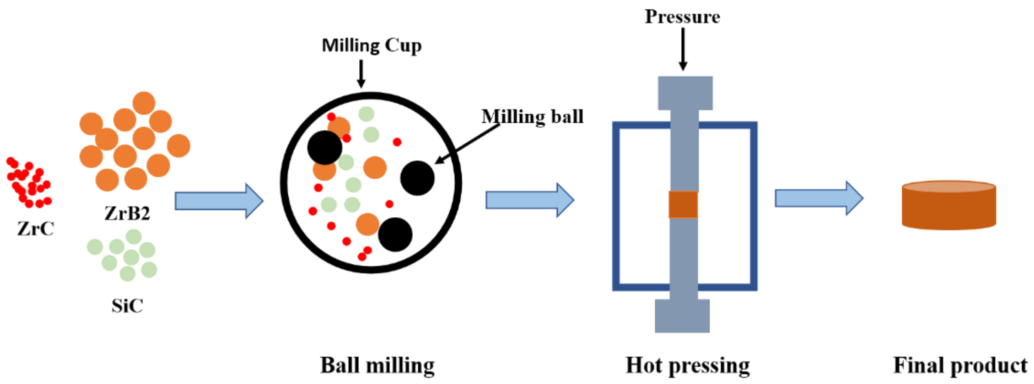

Fig. 2.3 The production steps of the ZrB_2-SiC-ZrC specimens via hot pressing

Reactive hot pressing:

Reactive hot pressing possesses a controlled reaction to form non-oxide ceramics. The solid-state reaction ensures the completely converted product is from the reactant. Precise reaction and application of pressure in a combined in-situ produces dense ZrB_2-based ceramics. The sintering temperature is minimized relative to conventional hot pressing due to the depreciation of oxide impurities such as B_2O_3 and ZrO_2. Finer particle size occurs by high-energy milling, which leads to a large defect concentration inside the precursor, resulting in densification. Chamberlain et al. [98] have reported a 99 % density of ZrB_2 ceramic by RHP at 2100°C. The properties of conventionally processed ceramics are comparable to those of hot-processed ceramics. The reactive hot pressing of attrition-milled Zr-B powder is mixed to produce nano-sized scale particles (less than 100nm). Due to tiny particle precursors, the controlled reaction takes place at 600°C. Furthermore, Liu et al. [139] fabricated fully dense ZrB_2 ceramic with less than 1.5 fine grain size at 1900°C by combining ZrB and B powder. The successive reaction (2.16-2.18) occurs between the powder mixture at various temperatures.

Peritectic decomposition of $2ZrB = ZrB_2 + Zr$ *at 1250°C* (2.16)

$ZrB_2 + Zr \rightarrow$ *Leu* (ZrB_2+Zr) *at 1661°C* (2.17)

Zr *in Leu* $(ZrB_2+Zr) + 2B = ZrB_2$ (2.18)

The monolithic ZrB_2 ceramic has unsatisfactory strength and oxidation resistance for ultra-high temperature applications. As a result, Zhang et al. [100] developed ZrB_2-SiC ceramic composites from Zr, Si, and B_4C starting powders, which are attrition milled and RHP under vacuum at 1900°C for 1 h. The powder is attrition milled for 1 h, forming a nano-sized ZrB_2 phase with improved densification and mechanical properties compared to conventional HP. Similarly, Wu et al. [114] developed ZrB_2-SiC-ZrC composite from Zr, Si, and B_4C as starting material to achieve 97% sinter-density at 1800°C. The formation of ZrC improves the densification during the sintering of the composite at low temperatures. The sintering temperature can be reduced from 1800 to 1600°C while attaining 97.3% sintering density using high-energy ball-milling of raw powder of ZrB_2-SiC-ZrC composites.

Table 2.3 The sintering pressure, sinter density, grain size, and mechanical properties of ZrB_2 and ZrB_2-based composite via hot Pressing

Materials Composition	Pressure (MPa)	sintering Condition	Microstructural Phases	Sinter-density (as% ρth)	Hardness (GPa)	Fracture Toughness (MPa m½	Flexural strength (Mpa	Refs.
ZrB_2 (RHP)	30	1900°C/ 45 min	ZrB_2	-	23.0	-	565	[140]
B_4C (1.3 µm), ZrO_2 (60 mesh)	30	2000°C/ 60 min	ZrB_2	95	25	-	400	[97]
Zr, B (RHP) (10nm)	40	2100°C/ 45 min	ZrB_2	99	-	-	434	[98]

ZrB$_2$ (2 µm)	32	2100°C /60 min	ZrB$_2$	97.01	13.7	3.1	392	[99]
		2150°C /30 min		96.74	13	3.2	398	
		2150°C /60 min		97.33	14.1	3	394	
		2150°C /120 min		97.81	14.4	2.7	337	
		2200°C /60 min		97.05	13.6	2.9	345	
Zr (43 µm), Si (10 µm), B$_4$C (1 µm)	30	1900°C/ 60 min	ZrB$_2$–SiC	97.67	21.0	4	506± 43	[100]
ZrB$_2$ (2 µm), SiC (0.7 µm)	32	1650-1900°C /60 min	ZrB$_2$	99.8	23	3.5	565	[101]
			ZrB$_2$-10 SiC	93.2	24	4.1	713	
			ZrB$_2$-20 SiC	99.7	24	4.4	1003	
			ZrB$_2$-30 SiC	99.4	24	5.3	1089	
ZrB$_2$ (3 µm), α-SiC (0.8 µm)	40-50	1900°C /20 min	ZrB$_2$ - 10 vol. % α-SiC	100		4.8	835	[102]
ZrH$_2$(2 µm), Si (3.5 µm) B$_4$C (0.8 µm)	30	1890°C /10 min	ZrB$_2$–27vol% SiC	98	22.6	3.5	720	[103]
ZrB$_2$ (3µm), SiC(1.1-2.5 µm)	26-30	1800-2150°C/ 40 min	ZrB$_2$–SiC	-	15-16	2-3.5	499	[105]
ZrB$_2$, (4.4 µm) SiC	32	1650/60 min	ZrB$_2$–30 vol.% SiC	-	21.4	-	1150	[107]
ZrB$_2$, (6.4 µm) SiC				-	21.7	-	924	
ZrB$_2$, (8.2 µm) SiC				-	21.2	-	892	
ZrB$_2$,(11.5µm) SiC				-	21.2	-	825	
ZrB$_2$,(11.8µm) SiC				-	19.3	-	724	
ZrB$_2$, (12 µm) SiC				-	18.6	-	460	
ZrB$_2$, (13 µm) SiC				-	18.4	-	280	

ZrB_2, (18 μm) SiC				-	17.3	-	245	
ZrB_2 (1.05 μm), SiC (0.45 μm)	30	1900°C /60 min	ZrB_2–20 vol% SiC	-	17.82	3.4	462	[108]
ZrB_2 (2 μm), SiC (2 μm)	10	2000°C/ 30 min	ZrB_2–15 vol% SiC	98.3	14.9 ±0.3	3.5± 0.1	-	[109]
		2000°C/ 30 min	ZrB_2–20 vol% SiC	98.8	16.9 ±0.3	3.8± 0.2		
		2000°C/ 30 min	ZrB_2–25 vol% SiC	99.3	19.6 ±0.1	4.5± 0.1		
		2000°C/ 30 min	ZrB_2–30 vol% SiC	99.8	21.3 ±0.4	4.7± 0.1		
ZrB_2 (2 μm), (2 μm) SiC	10	1700°C/ 30min	ZrB_2-20 vol % SiC	91	14			[110]
		1850°C/ 30min		96	18			
		2000°C/ 30min		99.9	21			
$ZrSi_2$(5μm), B_4C (2-3μm), C (40 nm)	40	1550°C /30 min	ZrB_2–SiC	97.6	17.1 ±0.7	6.08		[111]
Zr (25 μm), Si (50 μm), B_4C(2μm)	20	RHP, 1800°C/ 60 min	ZrB_2-SiC-ZrC	96.8	16.7	5.1	-	[113]
ZrB_2 (2μm),SiC(1μm), ZrC (2 μm)	30	HP1850°C/60 min in Ar	ZrB_2–SiC–ZrC	98.2	19.4 ± 0.4	5.65 ± 0.16	681± 67	[114]
Zr (40 μm), Si (40 μm), B_4C (8μm)	30	RHP 1000°C/ 60min 1500°C/ 60 min		99.1	20± 0.5	7.19 ± 0.20	654± 17	
Zr, Si, B4C	20	RHP, 1600°C/ 180 min	73.96 ZrB_2-21.04 SiC-5ZrC	97.3	17.2	5.2	747	[115]
ZrB_2 (1.05 μm) ,SiC (0.45 μm), ZrC(0.85 μm)	30	2000°C/ 180 min	ZrB_2-20SiC	100.2	19.3	3.89	562	[117]
			ZrB_2-10SiC-10ZrC	100.2	17.7	4.60	851	
			ZrB_2-20ZrC	100.1	16.3	4.48	794	
			ZrB_2-20 SiC-20 ZrC	99.8	18.4	4.84	785	

2.4.3 Spark plasma sintering

Spark plasma sintering is the most advanced technology to develop highly dense ZrB_2-based composite at lower temperatures and shorter times than conventional techniques. It is similar to the hot-pressing sintering method, but in hot pressing, indirect heating occurs rather than direct heating in spark plasma sintering. In the SPS technique, pulsed direct current hits the graphite die simultaneously at applied uniaxial pressure. The natural pulse creates a very high heating and cooling rate, which enhances grain growth and diffusion mechanism inside the composite. The high-intensity pulse direct current with low voltage and uniaxial pressure at a high heating rate of nearly 1000°C /min resulted in a highly dense ceramic structure [141]. Some researchers have reported that through the SPS technique, the completely densified composite (98.5 %) can be obtained at a very low temperature (1500-1900°C) and minimum time (5-20 min) with a smaller particle size shown in Table 2.3.

Oxygen contamination present in starting powder can create oxides such as B_2O_3 and ZrO_2, and this impurity limits the densification. But in SPS, pulsed current local and electrical discharge, which cleans the surface oxide and grain boundary diffusion, promotes the densification of ceramics. The surface temperature of the die is higher than the internal temperature of the specimen. This temperature mismatch has been affected by many factors, such as the size of the die, vacuum quantity in the chamber, conductivity and insulation level in the die, etc [118]. The SPS technique allowed dense materials to be obtained without the addition of sintering aids and in a shorter time than the HP technique. The typical duration of densification of the HP cycles was more than 2 h, while in the SPS process, it was completed in about 20 min [142]. At a high densification rate, some gaseous components (B_2O_3) have no time to escape and get encapsulated into the ceramics. Evaporation–condensation kinematics of B_2O_3 are the main factors in promoting the coarsening of ZrB_2-based ceramics. Rapid heating rate in the temperature range of 1500-1900°C and reducing the evaporation condensation time of B_2O_3 restricts the coarsening of ceramic.

In conclusion, a fast-heating rate reduces the adverse effects of grain coarsening of B_2O_3. Also, a grain boundary is enhanced due to the electric field supply, reducing porosity [118]. In the SPS process, the grain size of ZrB_2 particles is small due to the large CTE of ZrB_2, rapid heating rate, and high pressure at the beginning of sintering.

The oxidation resistance of ZrB_2-based composites is boosted by adding sintering aids in the form of particulate whiskers or a combination of both. Zhang et al. [125] have reported ZrB_2–SiC ceramics fabricated by spark plasma sintering at 1375°C for 5 min under a uniaxial load of 25 MPa. The flexural strength of ZrB_2–15 vol.% SiC ceramic was lower than that of ZrB_2–30 vol.% SiC ceramic due to a more significant amount of SiC. The flexural strength is increased due to SiC particles on the boundary of ZrB_2, enhancing the binding force between ZrB_2 particles. The weight loss and voids improved due to the rapid evaporation of SiO_2; thus, the ablation resistance decreased at 3000°C. An excess amount of SiC creates more flaws, making it harder to form a continuous layer to seal the defect, leading to the dissatisfactory resistance to ablation for the ZrB_2–30 vol.% SiC.

Recently, ZrB_2-ZrC-SiC-based composites have had superior mechanical, thermal, and electrical properties when consolidated via the SPS technique**.** Guo et al. [143] examined the properties of ZrC-ZrB_2-SiC-based composite sintered at 1950°C for 2 min under a pressure of 50 MPa. Depending on the compositions, the shear and Young's modulus were 180–225 GPa and 435–517 GPa, respectively. The range of hardness, fracture toughness, thermal conductivities, and electrical conductivities were 18.8–21.5 GPa, 4.6–6.1 MPa $m^{1/2}$, 38.25–92.85 W m^{-1} K^{-1} and 0.916–4.521 × 10^4 respectively. Similarly, Rezapour et al. [130] analyzed the effect of ZrC on fracture toughness and hardness of ZrB_2-SiC composites via SPS at 1800°C for 9 min and under a pressure of 30 MPa. Upon addition of ZrC up to 8 vol%, fracture toughness was increased from 4.8 MPa $m^{1/2}$ to 6.6 MPa $m^{1/2}$ but decreased to 5.9 MPa $m^{1/2}$ when added up to 12 vol%. Similarly, hardness increased up to 5 GPa and decreased further.

Reactive SPS

In the reactive SPS technique, the sintering temperature is reduced compared to SPS sintering due to particle size reduction through milling. Zhao et al. [123] fabricated ZrB_2–SiC composite by Zr, Si, and B_4C as starting materials via SPS reactive synthesis method at 1450°C for 3 min under 30 MPa. The density increases with holding time, but hardness decreases slightly due to grain growth. SPS is a suitable technique for preparing nanocomposites, as no grain growth occurs in this process. Nanocomposite ceramics have superior mechanical properties and good application prospects.

Table 2.4 The sintered density, grain size, and mechanical properties of ZrB_2 and ZrB_2-based composite via SPS

Materials Composition	Pressure MPa	sintering Condition	Phases	Sinter-density (as% ρth)	Hardness (GPa)	Fracture Toughness (MPa $m^{1/2}$	Flexural strength (GPa	Refs.
ZrB_2 (1.5–2.5 μm)	50	1900°C /3 min 200°C /Min	ZrB_2	97	-	-	-	[118]
	50	1900°C / 3 min 300°C /min		98	-	-	-	
ZrH_2(2.5 μm), B (0.8 μm)	50	1650°C / 10min	ZrB_2	89.9	-	-	333	[119]
		1700°C / 10min		93.4	-	-	351	
	50	1750°C / 10min		95	-	-	435	

	50	1800°C /10 min		97.2	-	-	491	
ZrB_2 (2 μm)	75	1900°C / 6 min	ZrB_2	90-96	-	-	-	[120]
ZrB_2	75	1625°C /12 min	ZrB_2	98.5	-	-	-	[121]
$ZrOCl_2.8H_2O$, H_3BO_3, gum karaya	50	1900°C / 10 min	ZrB_2	87-93	-	-	-	[122]
Zr (45μm), Si (50μm) B_4C (2μm)	30	RSPS 1450°C / 3min	ZrB_2-25 vol% SiC	98.5	17.18 ± 0.26	4.31 ± 0.20	-	[123]
ZrB_2, SiC	20	1800-1900°C/ 5min	ZrB_2-20-60% SiC	92-95	22-24	4.1	-	[124]
	10	2000-2100 °C / 3min		99	26.8	3.2-3.6	-	
ZrB_2(15 μm), SiC (0.55 μm)	25	1375°C /5min	ZrB_2–15 vol% SiC	93.1	10.5	-	335.5	[125]
	25		ZrB_2–30 vol% SiC	94.2	11.1	-	391.6	
ZrB_2, SiCp	50	1900°C /15min	ZrB_2-20 wt % SiCp	91.91	16.01	3.44	-	[126]
	50	2000°C /15min		91.95	16.22	3.69	-	
	50	2100◦C/15 min		93.04	14.32	3.61	-	
ZrB_2, SiC	50	1950°C /15 min	ZrB_2–17 vol% SiC	-	-	2.54± 0.29	585±88	[127]
	50		ZrB_2–32 vol% SiC	-	-	2.64± 0.27	552±59	
	50		ZrB_2–45 vol% SiC	-	-	2.90 ±0.34	751±81	
ZrB_2-ZrC-SiC	50	1950°C /2 min~400 ◦C/min	33.3ZrB_2-33.3 ZrC-33.3 SiC	98.7	19.1 ± 0.9	6.1 ± 0.7	-	[143]
	50		70ZrB_2-15 ZrC-15SiC	98.5	21.5 ± 1.3	6.0 ± 0.5		
	50		15ZrB_2-70 ZrC-15SiC	98.5	19.5 ± 1.0	4.6 ± 0.2		

	50		15ZrB_2-55 ZrC-30SiC	99.1	18.8 ± 0.7	5.5 ± 0.3		
	50		30ZrB_2-20 ZrC–50SiC	98.6	20.4 ± 1.9			
	50		55ZrB_2-15 ZrC–30SiC	98.7	19.6 ± 0.7	5.7 ± 0.4		
	50		55ZrB_2-30 ZrC–15SiC	98.8	19.4 ± 1.2	5.0 ± 0.3		
	50		30ZrB_2-55 ZrC–15SiC	98.5	19.6 ± 0.7	5.6 ± 0.2		

Microwave sintering

Microwave sintering is another alternative to conventional sintering, with uniform and rapid heating. In microwave sintering, the energy directly interacts with the material, resulting in higher energy efficiency. The heat is generated inside the specimen with microwave interaction [1][144]. Using microwave sintering, Zhu et al. [145] sintered ZrB_2-B_4C composite to sinter-density of ~99% theoretical density at 1820°C. The composite possesses a hardness of 17.5 GPa and fracture toughness of 2.8 $MPam^{1/2}$.

The rapid grain growth of the matrix is the main disadvantage of microwave sintering. Also, a non-uniform densification problem can be created by improperly optimized conditions. Thus, mechanical properties and physical properties have decreased.

2.4.4 Laser sintering

Laser sintering is the technique in which density is enhanced layer by layer from powder sintering. The cladding layer and 3D products for UHTC applications are produced using laser sintering. When the laser beam is incident on the composite surface, it absorbs the light energy, increasing temperature. Resultant grain growth occurs by the necking phenomenon, and partially or fully melting sometimes leads to densification. It is a non-contacting process, so the composite's contamination is minimal [145].

2. 5 Mechanical properties of ZrB_2-based composite

The mechanical properties of structural materials are crucial and fundamental for ultra-high temperature ceramics according to specific requirements. Various factors, such as processing techniques, incorporating sinter additives, phase evolution, and microstructure development, significantly impact these properties. Consequently, careful optimization becomes necessary. This section provides an overview of the parameters influencing the mechanical properties at room temperature. It will also highlight some successful endeavors that have showcased the potential for further enhancements through meticulous optimizations. Furthermore, it will explore the effects of sinter-additive contents/types (along with sinter-densities) on the mechanical properties of various UHTCs.

2.5.1 Fracture toughness

The fracture toughness is a demanding structural property for UHT structural applications. The fracture toughness of the ZrB_2 ceramics lies in the range of 2.4–4 MPa $m^{1/2,}$ and it increases with the addition of sintering additive up to 6.8 MPa $m^{1/2}$ as shown in Table 2.2, 2.3, and 2.4 for pressureless sintering, hot pressing, and SPS technique respectively. The low fracture toughness of ZrB_2 ceramics occurs due to cracks propagated across ZrB_2 grains and deflected along boundaries. In contrast, crack propagation along the boundaries is minimal for high fracture toughness. The intergranular cracking is dominant in the crack propagation along the grain boundaries. Therefore, intergranular cracking and more prominent grain are necessary for high fracture toughness. The metallic addition in ZrB_2-based ceramic enhanced grain growth compared to nitrides and carbides. However, metallic adding is more harmful in high-temperature applications due to the softer metallic bond responsible for the lower melting point. The nitrides and carbides have lower tensile residual thermal stress than metallic additives [146]. The hot-pressed ZrB_2 ceramics measured 3.5 (MPa.$m^{1/2}$) fracture toughness.

The fracture toughness increases with SiC addition due to crack deflection occurring near the SiC particles and interfaces of ZrB_2/SiC [101]. Rezaie et al. [147] investigated the particle size and distribution of SiC, which controls the fracture toughness of ZrB_2-based composites. The complex residual stress developed during cooling due to a mismatch of the thermal expansion coefficient of ZrB_2 and SiC particles, which most likely controlled the crack interaction.

The increase in fracture toughness depends upon crack deflection, crack deflection angle, or crack propagation path. The frictional and elastic bridging of grains also affects the fracture toughness. Flexible bridging is enhanced in larger-diameter grains, whereas smaller grains exhibit frictional bridging primarily due to grain pull-out and crack deflection. The fracture toughness of ZrB_2-based composites also depends upon the ratio of ZrB_2 to SiC grain size.

Recently, the toughness of the ZrB_2–ZrC–SiC composite reached ~6 MPa $m^{1/2}$ by optimizing the combination of composition with microstructure. Rezapour et al. [130] investigated the fracture toughness of ZrB_2-30 vol% SiC composites with different amounts of ZrC (4, 8, and 12 vol %) were SPSed at 1800°C for the time of 9 min. The result has shown the ZrC content increasing up to 8 vol%, fracture toughness was enhanced from 4.8 MPa $m^{1/2}$ up to 6.6 MPa $m^{1/2}$, but with more added up to 12 vol %, fracture toughness was decreased to 5.9 MPa $m^{1/2}$.

2.5.2 Flexural strength

Flexural strengths of the ZrB_2 ceramics with or without sinter-additives are shown in Tables 2.2, 2.3, and 2.4 for pressureless sintering, hot pressing, and SPS technique, respectively. ZrB_2 has exhibited better strength at room temperature in the 350 MPa to 580 MPa range. The flexural strength of the ZrB_2-based composite depends upon the particle size of the sintering additive and sintering parameters such as applied pressure, temperature, and sintering time. The hot-pressed monolithic ZrB_2 ceramics have 565 MPa flexural strengths at room temperature. For comparison, the flexural strength with pleasureless sintered ZrB_2 ceramics has 444 Mpa at room temperature with 98 % relative density [140]. The sintering time and temperature were also affecting the flexural strength. For example, the density of ZrB_2 ceramics was in the range of 96.74% (2150°C for 30 min) to 97.81% (2150°C for 120 min), and flexural strength ranged from 392 to 337 MPa, respectively. The larger grain size 52.1 μm and lower density (97.81%) show the lower strength value [139]. The main limitation of single-phase ZrB_2 ceramics is that it oxidized after 10 hours of sintering at 1400°C in air, and the loss of strength reached ~70%. However, this oxidation drawback has been removed by adding nano-sized SiC in ZrB_2 ceramic. Also, the flexural strength increases due to a thin oxide layer on the surface of the post-oxidized samples. The flaw healed without creating a new crack. The micron-sized SiC particle creates a thicker glassy layer on the surface, resulting in the defect forming at the interface between the oxide layer and decreasing strength [104]. Chamberlain et al. [101] showed that adding 10, 20, and 30 vol% SiC particulate in ZrB_2 Ceramics via hot pressing. With the addition of SiC particulate into the pure ZrB_2 matrix, the flexural strength increased from 565 to 1089 MPa at room temperature. F. Monteverde et al. [102] found that the effects of 10 vol. % ultra-fine (0.8 μm) α-SiC incorporation in ZrB_2 ceramic via hot-pressed at 1900°C for 20 min and 40–50 MPa of applied pressure at the room as well as at high-temperature. At room temperature, the flexural strength was 835 MPa, but with increasing temperature, at 1500°C, the flexural strength was 300 MPa. The addition of ultra-fine α-SiC particulate enhances the strength and oxidation resistance of ZrB_2. The mechanical properties of ZrB_2 are tested at 1450°C for 20 h. At this oxidizing condition, a borosilicate glassy phase has been formed on the surface of ZrB_2 ceramic to protect the hot environment. Further increased the temperature, a 64 % reduction occurred in initial strength. The morphology of SiC reinforcement is also an essential factor for enhancing flexural strength. Incorporating 15% vol SiC nanowhiskers into the ZrB_2 matrix enhances the densification and strengthens ZrB_2–SiCw composites, resulting in strengths ranging from 416 to 545 MPa [148]. Bellosi [142] et al. investigate the flexural strength of ZrB_2–ZrC–SiC composites at various temperature ranges. The flexural strength of the SPS sintered composite is 723 MPa, and the HP composite is 510 MPa at room temperature with a mean grain size of 2 μm.

2.5.3 Hardness

Hardness is an essential factor for structural application. Due to strong covalent bonding, ZrB_2 is an intrinsically complex material. When increasing the ionic bond in the basis bond, the hardness of ZrB_2-based composites decreases compared to ZrB_2-based ceramic. Like ZrB_2, various ceramics have covalent bonds with superior hardness (greater than 20 GPa) at room temperature [149]. The hardness of ZrB_2-based ceramic with or without additive varies in the 13-25 GPa range, as shown in Tables 2.2, 2.3, and 2.4. The additive/ reinforcement bonding and the amount of ceramics influence the sintered ceramic's hardness. The structural ceramic densification of the material should be nearly equal to the theoretical sintered density. The hardness of the ceramic depends upon the material's sintering density, which can be improved by adding additives [149,150]. The hardness of the composite is increased as its relative density increases.

The sinter density variation of ultra-high temperature ceramics depends upon the ceramic additive and its amount. With the addition of metallic additive in ZrB_2-based ceramic, the density of sintered ceramic is improved by liquid phase sintering. Still, the softer metallic bond decreases the hardness inside the sintered ceramic, which is more harmful in high-temperature applications [151,152]. In comparison, ceramic sintering additives in the ceramic matrix improved density and hardness for structural application at high temperatures.

Yan et al. [137] reported that ZrB_2-20 wt% SiC had 14.82 GPa Vickers hardness sintered by pressureless sintering, which is increased by 24 GPa when processed with hot pressing [101]. Mehdi et al. [109,110] prepared ZrB_2-30 vol% SiC composite by hot pressing at different processing temperatures (1700°C, 1850°C, and 2000°C) for 30 min. The densification of ZrB_2–30 vol% SiC composite increases (91-99%) with temperature, leading to increasing Vickers hardness from 15 GPa to 21.3 GPa because the residual pores could not withstand the stress applied by the indenter.

2. 6 High-temperature oxidation resistance

Analysis of oxidation behavior and resistance at ambient and high temperatures is essential for ultra-high temperature structural material. The oxidation rate and type depend upon the material density, temperature, partial pressure of oxygen, gas flow rate, particle size, and composite composition [153,154]. The oxidation behavior of ZrB_2 ceramics can be divided into two groups, depending upon the protective nature of the oxide layer. The low-temperature region is where the oxide layer is protected from oxidation, and the second one is the high-temperature region, where the oxide layer is not protected from oxidation. ZrB_2 ceramics exhibit good oxidation resistance due to the protective oxide layer at elevated temperatures. When ZrB_2 ceramics oxidize in air, ZrO_2 and B_2O_3 phases are formed, as shown in equation 2.19 [153].

$$ZrB_2 + 2.5O_2 \rightarrow ZrO_2 + B_2O_3 \qquad (2.19)$$

The amount of oxidized phase (ZrO_2 and B_2O_3) varies with temperature. Below 1000°C, the B_2O_3 glassy film forms on the top surface. In the ambient atmosphere, the B_2O_3 layer is a protective barrier toward oxygen diffusion, resulting in parabolic oxidation kinetics. But in between temperatures 1000-1800°C the mass gain occurs due to the formation of ZrO_2 and liquid B_2O_3, and mass loss exists due to volatilization of the protective B_2O_3 layer is high (illustrated in reaction 2.20), resulting in para-linear kinetics. The temperature range of 1000-1800°C has been attributed to the fast evaporation of B_2O_3 and leaving behind the non-protective ZrO_2 layer due to its porous nature. Various thermodynamic models have supported the oxidation behavior of ZrB_2 by volatility diagrams or kinetic models [155].

$$B_2O_3(l) \rightarrow B_2O_3(g) \text{ at above } 1100\ °C \tag{2.20}$$

Jin et al. [156] investigated the oxidation behavior of ZrB_2-based ceramic under compressive stress and temperature. The microstructural of the composite shows slow grain growth of ZrO_2 at 1000°C, but with increasing temperature, up to 1200°C, the growing rate is faster. The oxidation product ZrO_2 grain is converted to nano to micropore when the temperature exceeds 1400°C. When compressive stress (1 to 100 MPa) changes, the oxide layer thickness is almost the same, indicating no compressive stress effect on the oxidation rate. However, the microstructure of the composite is affected by compressive stress. The nanoindentation test shows excellent mechanical properties, such as young modulus (379.29 MPa) and hardness (16.79 MPa) at room temperature. Many researchers have reported that with the addition of SiC in monolithic ZrB_2-based ceramic, the linear oxidation resistance shifted to a parabolic growth rate at 1700°C. Additional benefits have been observed when SiC is incorporated into ZrB_2, even at ultra-high temperatures [157–166]. The following reaction (2.21-2.22) occurs during SiC addition in monolithic ZrB_2 at high temperatures.

$$SiC + 1.5O_2 \rightarrow SiO_2(l) + CO(g) \tag{2.21}$$

$$B_2O_3(l) + SiO_2 \rightarrow B_2SiO_3 + O_2 \text{ at above } 1100°C \tag{2.22}$$

In the ZrB_2-SiC system, three layers of borosilicate-based glasses have been formed: (i) B_2O_3 and SiO_2-based glassy layer, (ii) SiC-ZrO_2 based layer, and (iii) ZrB_2-SiC based layer [160]. The evaporation of B_2O_3 starts at 1200°C due to increasing vapor pressure. Still, a thin

SiO_2 layer has also been present on the surface up to 1500°C and provides a thermal barrier toward oxygen diffusion, resulting in continued protection. Below the SiO_2, ZrO_2-rich layers are present, and after that, SiC-depleted layers were observed. SiO_2 provides the oxidation resistance of ZrB_2-based composites by controlling the path, not ZrO_2 [160]. The oxygen diffusion coefficient of SiO_2 and ZrO_2 is 10^{-21} m^2/s and 10^{-10} m^2/s, respectively, at 1500 °C. Karlsdottir [162] et al. investigate the oxide scale formation on ZrB_2-15 vol% SiC ribbon specimen at 1700°C in the air for 15 min, at a heating rate of 480°C/min and free cooling (767°C/s). It consists of a thin silica layer, and a minor amount of SiO_2 is secure between the columnar ZrO_2 layer. Between the unreacted core and the ZrO_2 layer, a new region is called the SiC-depleted layer. The thickness of the SiC-depleted layer is 120 µm, and the consistency of the oxide scale was 102 µm. Guo et al. [104] reported the flexural strength of ZrB_2 nano and micro-based composites at room temperature and 1400°C for 10 hr in dry air for oxidation exposure. The nano-size ZrB_2-based composites have higher strength as compared to micro-size ZrB_2-based composites due to the uniform dispersion of SiC nanoparticles in grain and at the grain boundary. The micro size ZrB_2-based composites are located at multiple grain pockets. When a nano-sized particle of SiC is incorporated into ZrB_2-based ceramic then flexural strength is increased. In contrast, micro-size particle reduces the flexural strength of ZrB_2-based composites. Nano-sized SiC particles provide oxidation resistance due to the presence at intergranular and intragranular position resultant flexural strength improved.

Researchers report the oxidation resistance of ZrB_2-SiC-based composite with various parameters. Zhang et al. [167] fabricated ZrB_2-20 vol % SiC composite via crucible less-melting technique, and directional solidification improved oxidation resistance. The protective silica layer is formed on the specimen during solidification. Various studies have focused on selecting the optimum 20-30 vol% SiC composition for improving oxidation resistance. The high content of SiC provides oxidation resistance in the air at 1800°C due to a large amount of silica glass formation. The ZrB_2–SiC composite is thermally stable up to 1500°C, and the thickness of the oxidized layer is 100 µm. The borosilicate glass in the ZrB_2–SiC composite is dense with higher melting temperature, low oxygen diffusivity, and lower vapor pressure than liquid B_2O_3 in ZrB_2, which protects against oxidation. The formation of SiC depleted layer is suppressed by ZrC addition in ZrB_2-SiC based composite at different temperatures and pressures in various oxidizing conditions (air, ozone, hydrogen torch) [168,169].

Table 2.5 Oxide layer thickness, SiC depleted layer mass gain, and oxide phases of ZrB_2, ZrB_2-SiC, and ZrB_2–ZrC–SiC at different temperatures.

Material composition	Processing condition Temp/time (min)/pressure (MPa)	Oxidation condition	Oxide layer thickness (µm)	SiC depleted layer (µm)	Mass change (mg/cm2)	Ref
ZrB_2-20SiC	-	1327K;10 min	30	-	-	[157]
		1627K;10 min	150	100		
		1927K;10 min	1000	-		
ZrB_2–30 %SiC		1500°C;30min,	-	10	-	[158]
ZrB_2–15 %SiC	HP/ 1820/15/30	1450°C;1200 min	-	-	3.43	[159]
ZrB_2–30 vol.% SiC	HP/ 1950/20/32	1500°C,30 min	10	10	-	[160]
ZrB_2–20 vol.% SiC	HP/2000/60 /32	1800°C;0.2 atm	300	40	-	[161]
ZrB_2–20 vol.% SiC		1800°C;0.0002 atm	310	85		
ZrB_2–30 vol.% SiC		1800°C;0.2 atm	192	54		
ZrB_2–30 vol.% SiC		1800 °C; 0.0002 atm	380	220		
ZrB_2– 15 vol% SiC	-	1700°C; 15 min	102	120	-	[162]
ZrB_2–20 vol.% SiC	HP/ 1900/30/30	200Pa;1000°C; 30min	10	0		[163]
		200 Pa; 1200°C; 30min	72	37		
		200Pa;1400°C; 30min	40	25		
		200 Pa;1600°C; 30 min	160	50		

ZrB_2–80 vol.% SiC	SPS/2100/5/50	1773 K; 50 hr	490	None		[164]
ZrB_2–65 vol.% SiC	HP/1700/600/7		65	None		
ZrB_2–50 vol.% SiC			100	80		
ZrB_2–35 vol.% SiC			120	170		
ZrB_2–20 vol.% SiC			120	260		
ZrB_2–80 vol.% SiC	SPS/2100/5/50	2073 K for 20 min torch	-	None		
ZrB_2–65 vol.% SiC	HP/1700/600/7		-	None		
ZrB_2–50 vol.% SiC			-	110		
ZrB_2–35 vol.% SiC			-	160		
ZrB_2–20 vol.% SiC			-	170		
ZrB_2–10 vol.% SiC	HP/1950/60/30	1800°C; 200 s	65			[165]
ZrB_2–15 vol.% SiC		1800°C ;400s	70			
ZrB_2–30 vol.% SiC		1800°C; 600s	120			
ZrB_2–30 vol% SiC	HP/1950/120/32	1500°C; 100min	39.6	-	2.54	[166]
		1500°C; 100min, Polished	41.3		2.96	
$20ZrB_2$-16SiC-64ZrC	SPS/1950/2/50	1700°C; 10 min under oxygen-hydrogen combustion gas	175	-	-	[168]
$34ZrB_2$-16SiC-50ZrC			250			
$50ZrB_2$-16SiC-34ZrC			210			
$64ZrB_2$-16SiC-20ZrC			150			
ZrB_2-SiC			50			
ZrB_2-SiC	SPS/1950/2/50	2000°C;5-10 sec	50	-	-	[169]
$50ZrB_2$-16SiC-34ZrC			210			
$64ZrB_2$-16SiC-20ZrC			150			
ZrB_2-SiC			50			
ZrB_2–10 vol.% SiC	HP/2000/60/30	1500°C;0.5-10h	40-180	10-55	29.7	[170]
ZrB_2–30 vol.% SiC			10-25	10-15	3.9	
$20ZrB_2$-16SiC-64ZrC	SPS/1950/2/50	1700°C in the air; low oxygen partial pressure	180	-	-	[171]
$34ZrB_2$-16SiC-50ZrC			121			
$50ZrB_2$-16SiC-34ZrC			110			
$64ZrB_2$-16SiC-20ZrC			100			
ZrB_2-SiC			62	30	-	

2. 7 High-temperature ablation resistance

Ablation resistance is one of the most essential parameters UHTCs use in reusable space vehicles' thermal protection systems. Table 2.5 mentions the oxidation and ablation conditions for different compositions. The form of rigid surfaces must possess the ability to endure extreme heat, high heat flux, and mechanical stress induced by vibrations during launch and re-entry into the Earth's atmosphere. The mass ablation rate serves as a measure of weight change before and after ablation. In contrast, the linear ablation rate signifies the thickness alteration of the significant erosion zone on the ablation surface [172].

Arc jet testing is commonly employed to simulate atmospheric re-entry conditions and assess material behavior in hypersonic applications. Using arc-jet testing, Zhang et al. [173] investigated the ablating properties of hot-pressed ZrB_2-20 vol% SiC under simulated ground air re-entry conditions. They applied heat fluxes of 1.7 MW/m^2 and 5.4 MW/m^2 to the material. There was hardly any change in mass or shape after ablation in the higher heat flux condition when the surface temperature peaked at 1700°C. The ZrB_2-SiC composite, however, underwent considerable ablation at higher heat fluxes, with surface temperatures greater than 2300°C. Many literatures compared ZrB_2-SiC composite and C/SiC composite under simulated re-entry conditions, revealing that the ZrB_2-based composite exhibited superior thermal-oxidative and configurational stability. The 20% SiC ZrB_2 composite showed the most resistance to ablation compared to the other composites (10%, 20%, and 30% SiC). The 20% SiC ZrB_2 composite attributed to the material's advantageous thermal characteristics and sufficient Zr- and Si-oxide, which aided in the synthesis of $ZrSiO_4$ [174]. ZrO_2 and a liquid phase were produced due to the decomposition of $ZrSiO_4$ at high temperatures, successfully preventing oxidation. Zhang et al. [125] investigated the effects of SiC content (15 and 30 vol%) on the ablation behavior of ZrB_2 at 3000°C for 100 seconds. According to the findings, ZrB_2-15% SiC showed less oxidation and mass loss than ZrB_2-30% SiC. Also, it showed substantial mass loss and less creation of voids. In ZrB_2-15% SiC, the surface showed a continuous ablation layer with a speckled exterior and splashed inner regions. In contrast, a deep crater occurred at the center of the ablation region of ZrB_2-30% SiC.

2. 8 Research Gap

Limited studies on in situ synthesis: Although considerable efforts have been devoted to synthesizing ZrB_2-based composites, there is a research gap concerning the in-situ synthesis method. The in-situ approach involves the simultaneous formation of the composite phases during the synthesis process, resulting in improved homogeneity and enhanced properties. The investigation into the extensive validation of the synthesis process through X-ray Photoelectron Spectroscopy (XPS) analysis remains unclear. However, the literature lacks sufficient reports on the in-situ synthesis of ZrB_2-based composites.

Insufficient exploration of lower materials cost: Another research gap pertains to investigating ZrB_2-based composites with more inferior materials cost. Cost-effectiveness is a crucial factor for practical applications, and the synthesis of composites using cost-efficient materials has gained significant attention. However, there is a lack of comprehensive studies investigating the synthesis of ZrB_2-based composites with reduced material costs while maintaining desired properties.

Limited investigation of lower processing temperatures: Many existing studies have focused on synthesizing ZrB_2-based composites at high processing temperatures. However, there is a research gap regarding exploring synthesis methods to achieve the desired properties at lower processing temperatures. Lower processing temperatures can have several advantages, such as reducing energy consumption, enhancing safety, and expanding the range of compatible materials. Addressing this research gap is crucial for developing efficient and sustainable synthesis routes.

Need for simultaneous optimization of mechanical properties and resistance to ablation/oxidation: ZrB_2-based composites offer great potential for applications requiring excellent mechanical properties and resistance to ablation and oxidation at high temperatures. However, the existing literature lacks comprehensive studies that optimize these properties in ZrB2-based composites simultaneously. Bridging this research gap is essential for achieving multifunctional materials with enhanced performance in challenging environments.

The research gap in synthesizing ZrB_2-based composites can be attributed to the lack of literature on in situ synthesis with lower materials cost and processing temperatures while maintaining excellent mechanical properties and resistance to ablation and oxidation. Furthermore, the ablation properties of the in-situ formed ZrB_2-SiC composite, particularly under extreme conditions, such as high temperatures, have not been explored in prior research. The ablation properties add another layer of novelty to our thesis.

2. 9 The objective of the work

Ultra-High Temperature Ceramics (UHTCs) exhibit remarkable properties such as high melting points, excellent thermal stability, and exceptional mechanical strength, making them attractive for various applications, including aerospace, nuclear, and high-temperature engineering. Among UHTCs, ZrB_2 is a promising material due to its exceptional properties, including high melting point, low density, and high hardness. However, to further enhance its performance and expand its application range, researchers have explored the synthesis of binary and ternary composites by incorporating other ceramic phases such as SiC and ZrC.

Synthesize Binary and Ternary Composites:

- The extensive selection of high-purity precursor materials, meticulously assessing their characteristics. Choose ZrB_2, SiC, and ZrC precursor sources, ensuring their purity and compatibility with the targeted compositions.
- Develop precise stoichiometric ratios for the chosen precursor materials based on the desired compositions of the binary (ZrB_2-SiC, ZrB_2-ZrC) and ternary (ZrB_2-ZrC-SiC) composites. Optimize these ratios to balance phase distribution and enhance the final material properties.
- Precisely manipulate the synthesis conditions, including temperature reaction, duration, and gas atmosphere, to facilitate the desired reactions leading to the formation of binary and ternary composites.
- To optimize the microstructure and mechanical properties of the synthesized composites through heat treatment or sintering.

Physical and Structural Characterization:

- Conduct thorough physical and structural characterization of the synthesized composites.

- Utilize X-ray diffraction (XRD) techniques to analyze the composites' crystal structure and phase composition.
- Scanning electron microscopy (SEM) is used to examine the morphology, grain size, and distribution of the phases within the composites. Energy-dispersive X-ray spectroscopy (EDX) provides elemental analysis, ensuring the desired composition.
- XPS analysis is performed on the above sample to investigate and analyze the chemical composition and surface properties of the ZrB_2-based composite.

Mechanical Characterization:

- Perform comprehensive mechanical characterization of the synthesized composites.
- Measure properties such as hardness test to assess the resistance of the composites to indentation and deformation. Fracture toughness measurements determine the material's ability to resist crack propagation.
- Compare the mechanical properties of the composites with individual phases and relevant materials.

Application for Thermal Protection Systems and Ablative Applications:

- Evaluate the suitability of the synthesized composites for thermal protection systems.
- Assess the performance of the composites under high-temperature conditions.
- Investigate the resistance of the composites to ablation.

Overall, the objective of this thesis is to synthesize binary (ZrB_2-SiC and ZrB_2-ZrC) and ternary (ZrB_2-ZrC-SiC) composites, conduct physical and structural characterization, perform mechanical characterization, and evaluate their potential application for thermal protection systems and ablative applications.